

Accepted Manuscript

Discovery of novel [1,2,4]triazolo[4,3-a]quinoxaline aminophenyl derivatives as BET inhibitors for cancer treatment

Imran Ali, Jooyun Lee, Areum Go, Gildon Choi, Kwangho Lee

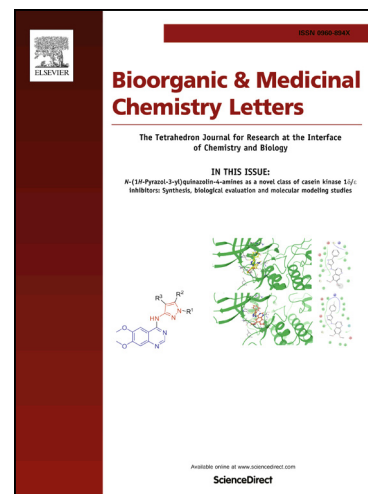
PII: S0960-894X(17)30921-6
DOI: <http://dx.doi.org/10.1016/j.bmcl.2017.09.025>
Reference: BMCL 25289

To appear in: *Bioorganic & Medicinal Chemistry Letters*

Received Date: 21 July 2017
Revised Date: 6 September 2017
Accepted Date: 12 September 2017

Please cite this article as: Ali, I., Lee, J., Go, A., Choi, G., Lee, K., Discovery of novel [1,2,4]triazolo[4,3-a]quinoxaline aminophenyl derivatives as BET inhibitors for cancer treatment, *Bioorganic & Medicinal Chemistry Letters* (2017), doi: <http://dx.doi.org/10.1016/j.bmcl.2017.09.025>

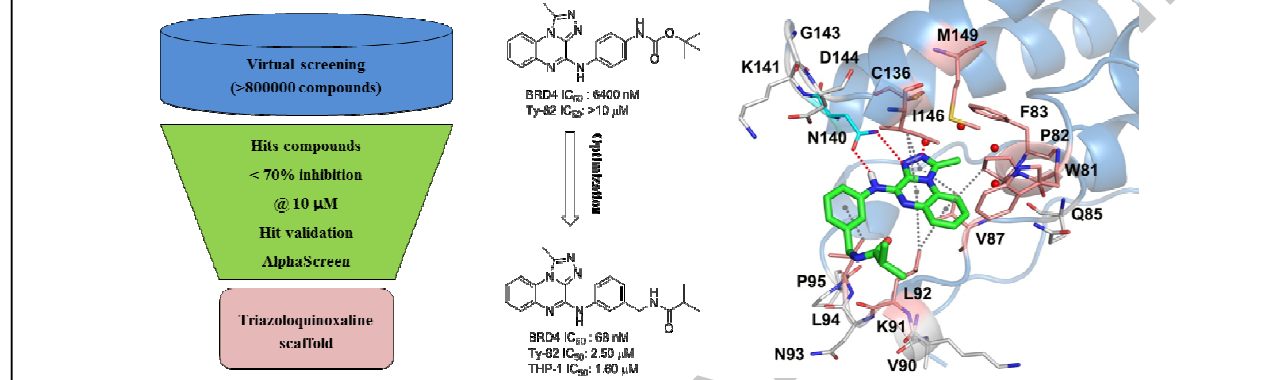
This is a PDF file of an unedited manuscript that has been accepted for publication. As a service to our customers we are providing this early version of the manuscript. The manuscript will undergo copyediting, typesetting, and review of the resulting proof before it is published in its final form. Please note that during the production process errors may be discovered which could affect the content, and all legal disclaimers that apply to the journal pertain.



Graphical Abstract

Discovery of novel [1,2,4]triazolo[4,3-a]quinoxaline aminophenyl derivatives as BET inhibitors for cancer treatment

Leave this area blank for abstract info.

Imran Ali^{a,b}, Jooyun Lee^a, Areum Go^{a,b}, Gildon Choi^{a,b,*}, Kwangho Lee^{a,b,*}



Discovery of novel [1,2,4]triazolo[4,3-a]quinoxaline aminophenyl derivatives as BET inhibitors for cancer treatment

Imran Ali^{a,b}, Jooyun Lee^a, Areum Go^{a,b}, Gildon Choi^{a,b*}, Kwangho Lee^{a,b*}

^aBio-Organic Science Division, Korea Research Institute of Chemical Technology, PO Box 107, Daejeon 34114, Republic of Korea.

^bMedicinal Chemistry & Pharmacology, Korea University of Science & Technology, Daejeon 34113, Republic of Korea.

Tel: +82-42-860-7176, Fax: +82-42-860-7160, e-mail: gchoi@kriict.re.kr, kwangho@kriict.re.kr

ARTICLE INFO

Article history:

Received
Revised
Accepted
Available online

Keywords:

Epigenetic readers
bromodomains
BET
BRD4
Triazoloquinoxaline
[1,2,4]triazolo[4,3-a]quinoxaline
cancer

ABSTRACT

Bromodomain and extra-terminal (BET) proteins, a class of epigenetic reader domains has emerged as a promising new target class for small molecule drug discovery for the treatment of cancer, inflammatory, and autoimmune diseases. Starting from *in silico* screening campaign, herein we report the discovery of novel BET inhibitors based on [1,2,4]triazolo[4,3-a]quinoxaline scaffold and their biological evaluation. The hit compound was optimized using the medicinal chemistry approach to the lead compound with excellent inhibitory activities against BRD4 in the binding assay. The substantial antiproliferative activities in human cancer cell lines, promising drug-like properties, and the selectivity for the BET family make the lead compound (**13**) as a novel BRD4 inhibitor motif for anti-cancer drug discovery.

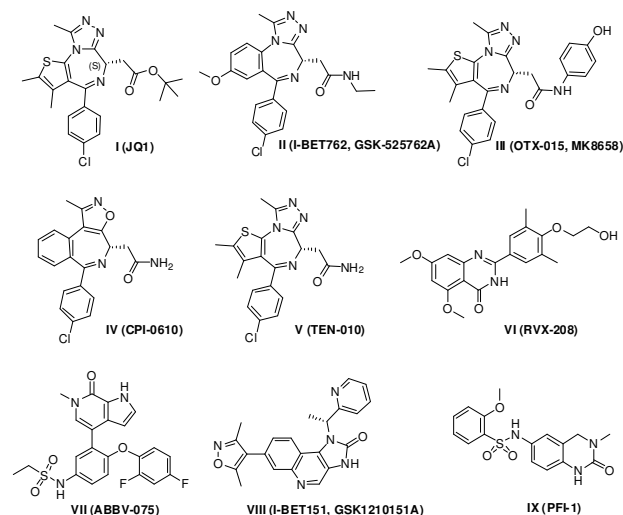
2009 Elsevier Ltd. All rights reserved.

Activation of transcription is modulated by acetylation of the lysine residues on histones. Lysine acetylation, a key post translational modification, is mediated by histone acetyltransferases (HATs) and results in the neutralization of positive charge on lysine side chains. Consequently, the histone-DNA interactions are altered and the diminished nucleosome compaction enhances the transcriptional activity by recruiting the transcription and chromatin remodeling factors which is mediated by *bromodomain containing proteins* (BRDs)¹. BRDs act as epigenetic readers by recognizing and binding to the acetylated lysine residues of the histone tails, thus regulating the key processes of gene transcription and gene expression^{2,3}. *Bromodomain and extra-terminal* (BET) proteins, a subfamily of human BRDs, is composed of four members (BRD2, BRD3, BRD4 and BRDT) in humans. BET proteins have two similar N-terminal bromodomains and an extra-terminal protein interaction motif at the C-terminus. Like all other BRDs, the BET family recognizes and binds to the acetylated lysine residues in histones H3 and H4⁴⁻⁷. BET proteins have been evidenced to be implicated in several human diseases such as MLL1-fusion leukemia, NUT midline carcinoma, various inflammatory diseases, and cardiovascular disorders⁸⁻¹¹.

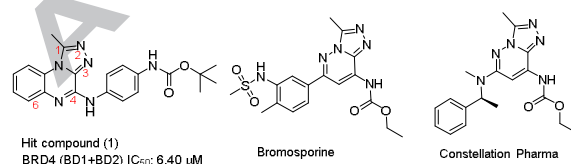
The structural design of the acetyl lysine binding pocket of BET proteins makes them attractive druggable targets for drug discovery campaigns. The architecture of the binding pocket has been reported to be favorable for the development of small

molecule inhibitors and a number of potent small molecule BET inhibitors have been reported up to date (Figure 1)^{12,13}. The rapid progress in the development of small molecule BET inhibitors have greatly stimulated the drug discovery efforts both from academia and pharmaceutical industry, and have led to more than a dozen BET inhibitors into the human clinical trials. Despite this enormous progress, there is still a need for new chemotypes with improved pharmacokinetics and physicochemical properties which will further increase our understanding of the therapeutic potential of the BET inhibitors for various human diseases¹⁴⁻¹⁸. Recently, JQ1 has been reportedly related to memory deficits in mice and the drug resistance against JQ1-motif triazoloazepines has been described¹⁹. These issues further provide a strong demand for the development of additional chemotypes for BET inhibitors. The new chemotypes are thus strongly desirable as alternatives for the clinical developments.

In the present work, we unveil the discovery of novel [1,2,4]triazolo[4,3-a]quinoxaline aminophenyl derivatives as potent BET inhibitors. Discovery from virtual screening and the medicinal chemistry optimization of the hit compound to the lead has been described. Biological evaluation of a new class of potent and orally bioavailable BET inhibitors as anticancer agents has been thoroughly discussed as well.

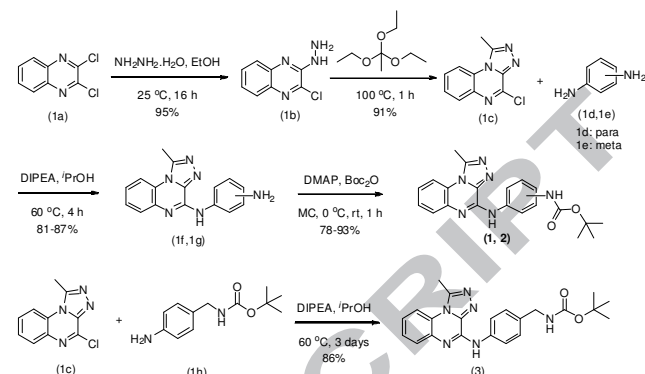
Figure 1. Representative BET inhibitors

All the molecular modeling was carried out using the Maestro v10.2 (Schrödinger, Inc.)²⁰. In an effort to discover BET inhibitors with a novel scaffold, the docking based high throughput virtual screening was performed using the fragment-like database²¹ with more than 800,000 compounds from ZINC²² and the X-ray crystal structure of BRD4 (PDB id: 4CLB)²³. Starting the molecular modeling, four water molecules located within the binding pocket were considered to be conserved in the majority of bromodomains. The structural defects of the protein were fixed by the Protein Preparation Wizard. The low-energy 3D structures of compounds were generated by the LigPrep, and then they were docked into the binding pocket of BRD4 using the Glide in Standard Precision (SP) mode based on a grid box of $20 \times 20 \times 20 \text{ \AA}^3$ centered on the co-crystallized ligand. We used constraints such as H-bond interactions with the side-chain of Asn140 and water molecule. The docking results were ranked and filtered by the Glide score. The top 2000 poses were clustered according to structural similarity, and finally 8 fragment-like motifs were selected. 230 Compounds having 8 fragment-like motifs were obtained and tested for the inhibitory activity against BRD4. The active BET inhibitors with [1,2,4]triazolo[4,3-a]quinoxaline scaffold were docked into the binding pocket of each BD1 (PDB id: 4CLB) and BD2 (PDB id: 2YEM²⁴) of BRD4 using the Glide in Extra Precision (XP) mode. Other options were the same as mentioned above. The protein-ligand interactions were analyzed by the Discovery Studio Modeling Environment v4.0²⁵ and the molecular models of the docked compounds were displayed using the PyMOL software²⁶.

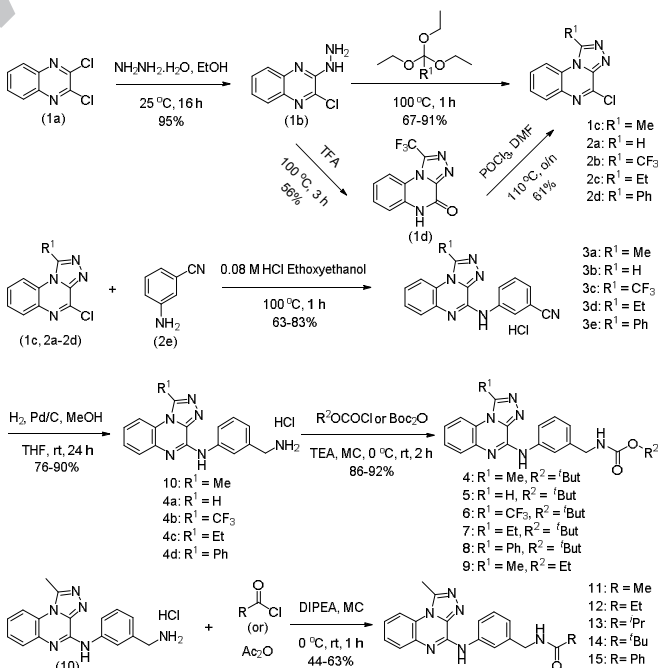
Figure 2. Discovery of hit compound **1** by virtual screening

The virtual screening hit compound **1** shown in Figure 2, based on a novel [1,2,4]triazolo[4,3-a]quinoxaline motif, was validated by IC₅₀ measurement using the AlphaScreen binding assay²⁹. A careful survey of the literature revealed bromosporine, a triazolopyridazine based pan bromodomain inhibitor with very weak cellular potency²⁷. A patent from Constellation

Pharmaceuticals have also described a series of BET inhibitors based on triazolopyridazine scaffold²⁸. Putting all together, the newly discovered triazolo quinoxaline scaffold seemed to be a good starting point for the search of more potent and selective BET inhibitors.

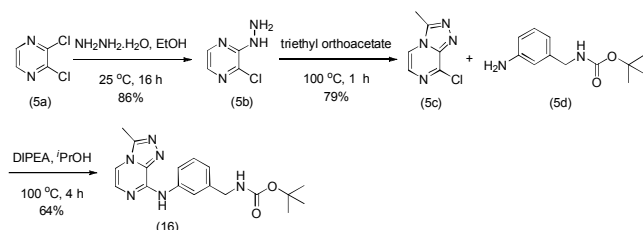
**Scheme 1.** Syntheses of compound **1-3**

Compound **1-3** (Table 1) were prepared by the synthetic route described in Scheme 1. Addition of hydrazine monohydrate to the commercially available 2,3-dichloroquinoxaline (**1a**), followed by cyclization with triethyl orthoacetate afforded 4-chloro-1-methyl triazoloquinoxaline core (**1c**) in excellent yield. Base-catalyzed coupling of *para*-phenylenediamine (**1d**) and *meta*-phenylenediamine (**1e**) with **1c** produced intermediates **1f** and **1g**, respectively. Installation of *tert*-butyloxycarbonyl (Boc) group to **1f** and **1g** furnished compounds **1** and **2**, respectively. Base catalyzed coupling of 4-(*N*-Boc-aminomethyl)aniline (**1h**) with key intermediate **1c** afforded compound **3** in 86% yield.

**Scheme 2.** Syntheses of compounds **4-15**

Compounds **4-15** (Table 1 & 2) were prepared according to Scheme 2. Various orthoesters were used to synthesize C-1 variants of the triazoloquinoxaline with chlorine at C-4 position (**1c**, **2a**, **2c**, **2d**). In case of CF₃ analogue at C-1 position of the triazoloquinoxaline ring, trifluoroacetic acid was used under reflux conditions, followed by chlorination of the resulting intermediate **1d** with phosphorous oxychloride provided the desired C-1 analogue **2b**. 3-Aminobenzonitrile was then coupled

with **1c** and **2a-2d** under acid catalyzed conditions using 0.08 M HCl in ethoxyethanol at 100 °C for one hour to furnish various nitriles (**3a-3e**). The resulting nitriles were reduced to the corresponding amines by employing palladium catalyzed hydrogenation (**10, 4a-4d**). Transformation of the resulting benzylamines to various carbamates and amides furnished compounds **4-9** and **11-15**, respectively.



Scheme 3. Synthesis of 3-methyl-[1,2,4]triazolo[4,3-a]pyrazine **16**

The synthesis of 3-methyl-[1,2,4]triazolo[4,3-a]pyrazine **16** is described in Scheme 3. Addition of hydrazine monohydrate to 2,3-dichloropyrazine, followed by cyclization with triethyl orthoacetate afforded **5c**. The base catalyzed coupling of **5c** with **5d** produced the desired compound **16** in 64% yield.

Table 1. C-1 and C-4 SAR of triazoloquinoxaline scaffold

R ¹	R ²	^a BRD4 IC ₅₀ (μM)	Ty-82 IC ₅₀ (μM)	THP-1 IC ₅₀ (μM)	
1		Me	6.40	>10	ND
2		Me	0.12	>10	ND
3		Me	2.70	>10	ND
4		Me	0.017	7.10	3.40
5		H	>10	ND	ND
6		CF ₃	>10	ND	ND
7		Et	>10	ND	ND
8		Ph	>10	ND	ND
I-BET762	-	-	0.061	0.39	0.29
OTX-015	-	-	0.016	0.067	0.033

^a: BRD4 IC₅₀ (BD1 + BD2)
ND: Not Determined

Compound **1**, discovered by virtual screening, exhibited modest BRD4 inhibitory activity of 6.40 μM in AlphaScreen assay. In order to design more potent derivatives, we planned to

carry out SAR studies at the amino phenyl ring attached at the C-4 position of the triazoloquinoxaline scaffold. The SAR of C-1 position of the triazoloquinoxaline scaffold was explored as well (Table 1). The meta-analogue **2** was significantly more potent (>50 fold) in the biochemical assay but lacked cellular potency. Introduction of methylene linker (entry **3**) boosted the biochemical potency but still lacked the cellular potency against Ty-82, a human NUT midline carcinoma cell line. Delightfully, the meta-analogue **4** exhibited BRD4 inhibitory activity comparable with the reference compounds I-BET762 and OTX-015 in biochemical assay, and showed appreciable *in vitro* cellular potency against Ty-82 and THP-1 (human leukemic cell line). These observations confirmed that the methylene linker is essential for the potent BET inhibition. SAR exploration at the C-1 position of the triazoloquinoxaline revealed that methyl was the optimal substitution at this position. All other analogues having H, CF₃, ethyl, and phenyl group at C-1 position proved to be inactive in biochemical assay (**5-8**).

Table 2. Detailed C-4 SAR of triazoloquinoxaline scaffold

R	^a BRD4 IC ₅₀ (μM)	Ty-82 IC ₅₀ (μM)	THP-1 IC ₅₀ (μM)	
4		0.017	7.10	3.40
9		0.16	>10	>10
10	H	0.35	>10	ND
11		0.53	>10	ND
12		0.20	7.60	ND
13		0.068	2.50	1.60
14		0.097	>10	ND
15		0.64	8.60	ND
I-BET762	-	0.061	0.39	0.29
OTX-015	-	0.016	0.067	0.033

^a: BRD4 IC₅₀ (BD1 + BD2)
ND: Not Determined

With compound **4** as a potent BRD4 inhibitor, the drug-like properties of this lead compound were examined. Accordingly the liver microsomal stability and pharmacokinetic parameters of **4** were investigated and it was observed that **4** have low liver microsomal stability in mouse and rat while acceptable stability in human liver microsomes *in vitro* (Table 4 & 5). The inferior cellular potency and sub-optimal rat pharmacokinetic parameters of the **4** demanded for further optimization.

Further SAR analysis revealed that hydrophobic group is essential at the benzylamine end (Table 2). When the bulky and hydrophobic tertiary butyl carbamate (Boc) group was removed, the potency was diminished and this observation was in agreement with the docking studies (*vide infra*). Small-sized substitutions such as acetyl and ethyl carbamates were not tolerated. After thorough investigation, it was established that isobutyryl amide **13** was the substitution of choice. Replacement of the tertiary butyl carbamate (Boc) with isobutyryl amide not only boosted the cellular potency but also improved the pharmacokinetic parameters of the triazoloquinoxaline scaffold (Table 4 & 5).

Table 3. Role of quinoxaline phenyl ring

Structure	^a BRD4 IC ₅₀ (μM)	Ty-82 IC ₅₀ (μM)
4	0.068	2.50
16	1.50	>10

^a: BRD4 IC₅₀ (BD1 + BD2)

Finally, the role of the quinoxalinic phenyl ring was investigated. Changing the core from the quinoxaline to benzene-missing pyrazine **16** resulted in a considerable loss in biochemical potency and cellular activity (Table 3). This observation can be attributed to the loss of the protein-triazoloquinoxaline ligand hydrophobic interactions and was consistent with the docking studies (*vide infra*).

Table 4. *In vitro* liver microsomal stability of compound **4** and **13**

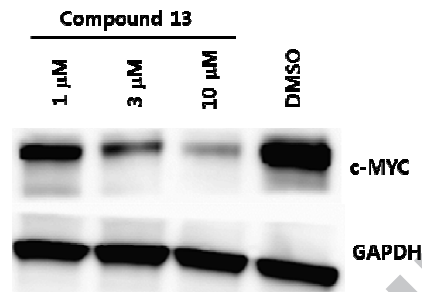
Compound	MLM % remain ^a	RLM % remain ^a	HLM % remain ^a
4	0.12	0.19	27
13	0.024	5	92

^a: percent remaining after 30 minutes of incubation.

Table 5. Pharmacokinetic parameters of compound **4** and **13** in rat

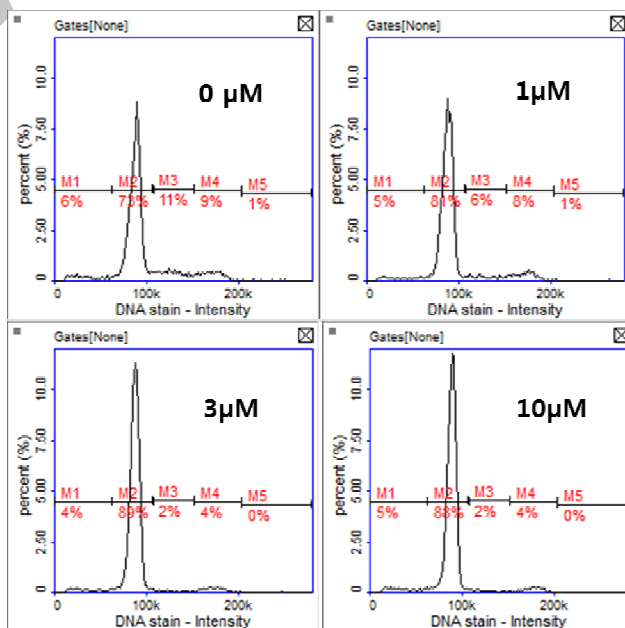
parameters	4 IV, 2mg/kg	4 PO, 5 mg/kg	13 PO, 20 mg/kg
T _{max} (hr)	-	3.42	1.3
C _{max} (mg/mL)	-	0.34	4.6
T _{1/2} (hr)	0.72	3.69	3
AUC _t (ug.hr/mL)	4.02	2.11	20.6
AUC _∞ (ug.hr/mL)	4.02	2.39	25.3
CL (L/kg/hr)	0.50	-	-
V _{ss} (L/kg)	0.46	-	-
F(%)	-	20.9	-

Figure 3. Western blot of the lysates from Ty-82 cells treated with compound **13** for 24 hr. The expression levels of c-MYC were found to be decreased in a dose-dependent manner upon the compound treatment



Recent studies of BET bromodomain inhibition identified a significant decrease in c-Myc expression with concomitant depletion of BRD4 at the Myc promoter in several cancer cell lines³⁰⁻³². The oncogenic transcription factor c-Myc is well known to control a gene expression program mediating cellular proliferation, metabolic adaptation, and survival. Thus, we can hypothesize that compound **13** treatment should decrease c-Myc expression in Ty-82 cell line. In fact, when the cells were treated with compound **13** for 24 h, c-Myc expression was found to be decreased in a dose-dependent manner as revealed by Western blot analysis³³ (Figure 3).

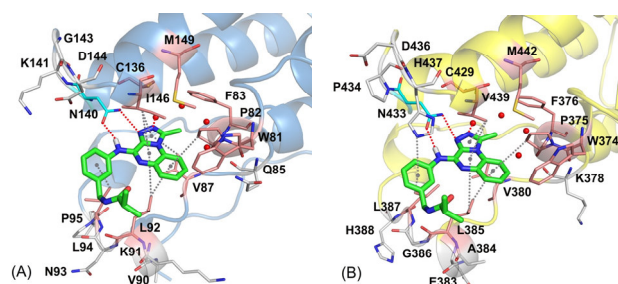
Figure 4. Cell cycle arrest induced by compound **13** in Ty-82 cells. DNA content histograms were recorded after treating the cells with various concentrations of compound **13** for 24 h. The G₁ population (M2) was found to be increased upon treatment of the compound from 73% (0 μM) to 88% (10 μM). M1: sub-G₁ phase, M2: G₁ phase, M3: S phase, M4: G₂/M phase, M5: miscellaneous



The eukaryotic cell cycle is traditionally divided into four phases: G₁, S, G₂ and M. G₁ represents the gap between M phase (M for mitosis) and S phase (S for DNA synthesis), while G₂ is the gap between S phase and M phase. It has been reported that genetic knockdown of BRD-NUT in NUT midline carcinoma cell lines such as Ty-82 results in terminal squamous cell differentiation and G₁ cell cycle arrest. The cytotoxic effects of compound **13** on Ty-82 cell line were investigated by cell cycle assays³⁴ whether the compound could inhibit the BRD4 activity and induce G₁ cell cycle arrest in the cell line. The cells were

treated with compound **13** for 24 h and labeled by cell-permeable nucleic acid stain for cell cycle analysis. The histograms in Figure 4 showed that compound **13** induced accumulation of Ty-82 cells in G₁ phase. Cell population in G₁ phase exposed to compound **13** (81% for 1 μ M, 89% for 3 μ M, and 88% for 10 μ M) was found to be significantly higher than the control cells (73%), strongly indicating that the cells are undergoing G₁ cell cycle arrest due to BRD4 inhibition by the compound.

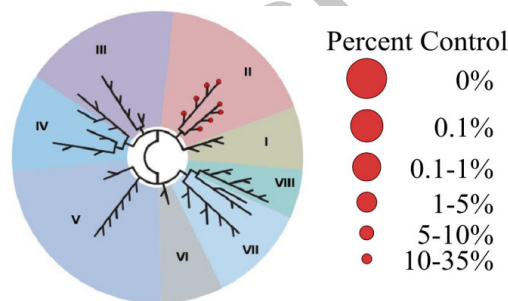
Figure 5. (A) Proposed binding mode of compound **13** (green stick) to the BD1 of BRD4: The key residues are represented by sticks, which of colors are different according to their interactions types such as hydrophobic (salmon) and H-bond (cyan). The different residues between binding pockets of BD1 and BD2 are represented by white sticks. The important waters are represented by red spheres. The H-bond and hydrophobic interactions are drawn as dashed red and gray lines, respectively. (B) Proposed binding mode of compound **13** (green stick) to the BD2 of BRD4: The key residues are represented by sticks, which of colors are different according to their interactions types such as hydrophobic (salmon) and H-bond (cyan). The different residues between binding pockets of BD1 and BD2 are represented by white sticks. The important waters are represented by red spheres. The H-bond and hydrophobic interactions are drawn as dashed red and gray lines, respectively



An insight of the binding interaction of **13** with BRD4 was examined by molecular docking. Compound **13** was docked with BRD4 and the docking result revealed the key interactions between **13** and the acetyl-lysine binding pocket of the BRD4. Compound **13** binds to the acetyl-lysine recognition pockets of both BD1 and BD2 of BRD4, which means that compound **13** recognizes common features of two bromodomains. The binding modes of compound **13** to BD1 and BD2 of BRD4 and their key interactions revealed by docking studies are shown in the Figure 5(A) & 5(B), respectively. The N3 atom on the [1,2,4]triazolo[4,3-a]quinoxaline forms H-bond interactions with the side-chain of Asn140 and the N2 atom interact tightly into nearby water molecule as depicted in Figure 5(A). The amine group at the C4 position of [1,2,4]triazolo[4,3-a]quinoxaline also forms the H-bond interaction with the side-chain of Asn140. The methyl group at the C1 position is located in the small hydrophobic pocket formed by Pro82, Phe83, Val87, and Ile146. The [1,2,4]triazolo[4,3-a]quinoxaline scaffold lies in the hydrophobic pocket formed by Pro82, Val87, Leu92, Cys136, and Ile146, and accepts alkyl- π interactions with the residues. The benzene ring of amino benzene substituent at the C4 position makes an alkyl- π interaction with Leu94. In particular, the isobutyryl amide group on the meta-position of benzene ring locates adjacent to the hydrophobic region named as the WPF shelf including Trp81, Pro82, Phe83, Ile146 and Met149, which improves its inhibitory activity against BRD4. Compound **13** binds to the acetyl-lysine recognition pocket of BD2 as well. The binding mode and key interactions of compound **13** in the BD2 is identical with those of compound **13** in the BD1 except an additional interaction between the amino benzene ring at the C4 position of [1,2,4]triazolo[4,3-a]quinoxaline scaffold and His437 as shown in Figure 5(B). As a result, compound **13** recognizes common features of two bromodomains.

Compound **13** was screened for its bromodomain selectively using BROMOscan™ service from DiscoverX. The TREEspot™ interaction map for compound **13** at a concentration of 500 nM is shown in Figure 6. Compound **13** TREEspot™ interaction map revealed that compound **13** is selective for the BET family of the bromodomains. **13** was found to be a pan inhibitor within the BET family inhibiting both BD1 and BD2 binding domains of all the four members of the family. This observation was confirmed by the similar K_d values between the two bromodomains of BRD4 (K_d values for BRD4(BD1) and BRD4(BD2) were 27 nM and 9 nM, respectively). No significant interaction was observed with other members of the bromodomain family at a concentration of 500 nM³⁵.

Figure 6. Bromodomain selectivity profiling of compound **13** with BROMOscan™ technology (DiscoverX, Inc.). The subclass II represents BET family. Measurements were performed at a concentration of 500 nM of the compound. The affinity was defined with respect to a DMSO control



In conclusion, we identified novel [1,2,4]triazolo[4,3-a]quinoxaline scaffold as BET inhibitors. An extensive SAR of the [1,2,4]triazolo[4,3-a]quinoxaline scaffold has been described. Compound **4** exhibited comparable biochemical potency with IBET-762 and OTX-015 with inferior cellular potency. Further optimization of compound **4** afforded compound **13** with improved cellular potency and pharmacokinetic parameters. An insight into the binding mode of compound **13** with BRD4 has been described. Novel [1,2,4]triazolo[4,3-a]quinoxaline scaffold along with anti-proliferative activity and drug-like properties makes compound **13** a promising lead for anticancer drug discovery. Efforts toward further optimization of compound **13** are underway and will be reported in due course.

Acknowledgments

The authors greatly acknowledge the generous financial support from the Bio & Medical Technology Development Program of the National Research Foundation funded by the Korean government (NRF-2012M3A9C1053340), the Korea Research Institute of Chemical Technology (KK1703-B01) and Korea Chemical Bank (SI1707-04).

References and Notes

- Elena F, Carlo P, Charles EM. Bromodomains: Structure, function and pharmacology of inhibition. *Biochem Pharmacol.* 2016;106:1-18.
- Arrowsmith CH, Bountra C, Fish PV, *et al.* Epigenetic protein families: a new frontier for drug discovery. *Nat Rev Drug Discovery.* 2012;11:384-400.
- Belkina AC, Denis GV. BET domain co-regulators in obesity, inflammation and cancer. *Nat Rev Cancer.* 2012;12:465-77.
- Filippakopoulos P, Piccaud S, Mangos M, *et al.* Histone recognition and large-scale structural analysis of the human bromodomain family. *Cell.* 2012;149(1):214-31.

5. Müller S, Knapp S. Discovery of BET bromodomain inhibitors and their role in target validation. *Med Chem Comm.* 2014;5(3):288-96.
6. Moriniere J, Rousseaux S, Steuward U, *et al.* Cooperative binding of two acetylation marks on a histone tail by a single bromodomain. *Nature.* 2009;461(7264):664-8.
7. Vidler LR, Brown N, Knapp S, *et al.* Druggability analysis and structural classification of bromodomain acetyl-lysine binding sites. *J Med Chem.* 2012;55(17):7346-59.
8. Filippakopoulos P, Qi J, Picaud S, *et al.* Selective inhibition of BET bromodomains. *Nature.* 2010;468:1067-73.
9. Dawson MA, Prinjha RK, Dittmann A, *et al.* Inhibition of BET recruitment to chromatin as an effective treatment for MLL-fusion leukaemia. *Nature.* 2011;478:529-33.
10. Nicodeme E, Jeffrey KL, Schaefer U, *et al.* A. Suppression of inflammation by a synthetic histone mimic. *Nature.* 2010;468:1119-23.
11. Anand P, Brown JD, Lin CY, *et al.* BET bromodomains mediate transcriptional pause release in heart failure. *Cell.* 2013;154:569-82.
12. Paul B, Panagis F, Stefan K. The therapeutic potential of acetyl-lysine and methyl-lysine effector domains. *Drug Discov Today: Ther Strateg.* 2012;9:e101-10.
13. Chun-wa C, David FT. Bromodomains: a new target class for small molecule drug discovery. *Drug Discov Today: Ther Strateg.* 2012;9:e111-20.
14. Jean-Marc G, Philip PS, Christopher JB. BET bromodomain inhibitors: a patent review. *Expert Opin Ther Patents.* 2014;24(2):185-99.
15. Xiaoqian X, Yan Z, Zhaoxuan L, *et al.* Discovery of Benzo[cd]indol-2(1H)-ones as Potent and Specific BET Bromodomain Inhibitors: Structure-Based Virtual Screening, Optimization, and Biological Evaluation. *J Med Chem.* 2016;59:1565-79.
16. <https://clinicaltrials.gov/> accessed on May 24, 2017.
17. Zhiqing L, Pingyuan W, Haiying C, *et al.* Drug Discovery Targeting Bromodomain-Containing Protein 4. *J Med Chem.* ASAP, 2017, DIO:10.1021/acs.jmedchem.6b01761.
18. Jonathan S, Yann L, Frédéric D, *et al.* Identification of a novel series of BET family bromodomain inhibitors: Binding mode and profile of I-BET151 (GSK1210151A). *Bioorg Med Chem Lett.* 2012;22:2968-72.
19. Alex MA, Laura MLH, Ryan JH, *et al.* BET Bromodomain Inhibitors with One-Step Synthesis Discovered from Virtual Screen. *J Med Chem.* 2017;60:4805-17.
20. Maestro, version 10.2; Schrödinger, LLC.: New York, NY, 2015.
21. Carr RA, Congreve M, Murray CW, *et al.* Fragment-based lead discovery: leads by design. *Drug Discov. Today.* 2005;10:987-92.
22. Irwin JJ, Shoichet BK. ZINC-A Free Database of Commercially Available Compounds for Virtual Screening. *J. Chem. Inf. Model.* 2005;45:177-82.
23. Atkinson SJ, Soden PE, Angell DC, *et al.* The structure based design of dual HDAC/BET inhibitors as novel epigenetic probes. *Med. Chem. Comm.* 2014;5:342-51.
24. Chung C, Coste H, White JH, *et al.* Discovery and Characterization of Small Molecule Inhibitors of the BET Family Bromodomains. *J. Med. Chem.* 2011;54:3827-38.
25. Discovery Studio Modeling Environment, version 4.0; Accelrys Software, Inc.: San Diego, CA, 2013.
26. The PyMOL Molecular Graphics System, version 1.7.4 Schrödinger, LLC. <http://www.pymol.org>.
27. Bromosporine (BSP). <http://www.thesgc.org/chemical-probes/Bromosporine>, accessed July 11, 2017.
28. Brian KA, Jean-Christophe H, Alexandre C, *et al.* Bromodomain inhibitors and uses thereof. *WO 2012174487*, 2012.
29. Measurement of the interaction between BRD4 and histone peptide was performed by utilizing the AlphaScreen technology provided by Perkin-Elmer. Purified BRD4 proteins containing two bromodomains were incubated with the tetraacetylated histone peptide (Anaspec., Inc.). The final concentrations of BRD4 and histone peptide were all 100 nM. BRD4 proteins and the histone peptide were added to the wells and incubated on ice for 2 hrs. Subsequently, nickel chelate acceptor beads and streptavidin coated donor beads (PerkinElmer) were added to the mixture and incubated for the additional 30 minutes at room temperature. The changes in alpha signal were read in alpha mode using a Fusion alpha-FP (Packard).
30. Mertz, JA, Conery AR, Bryant BM, *et al.* Targeting MYC dependence in cancer by inhibiting BET bromodomains. *Proc Natl Acad Sci U S A.* 2011;108:16669-74.
31. Ott CJ, Kopp N, Bird L, *et al.* BET bromodomain inhibition targets both c-Myc and IL7R in high-risk acute lymphoblastic leukemia. *Blood.* 2012;120:2843-52.
32. Zuber J, Shi J, Wang E, *et al.* RNAi screen identifies Brd4 as a therapeutic target in acute myeloid leukaemia. *Nature.* 2011;478:524-8.
33. For immunoblotting, cells were grown at 70% confluency in 6 well plates, treated with different concentrations of compound and incubated for 24 hr. The cells were washed with PBS and lysed with RIPA solution (50 mM Tris-HCl, pH 8.0; 150 mM NaCl; 1% NP-40; 0.5% sodium deoxycholate; 0.1% SDS). After heating the lysates for denaturation, the samples were electrophoretically separated on a 12% SDS-polyacrylamide gel. Proteins were transferred onto nitrocellulose membranes. Membranes were blocked with PBS containing 1% BSA and 0.1% Tween 20, pH 7.4 for 1 hr and then incubated sequentially with primary and secondary antibodies diluted in blocking buffer. Protein bands were detected with chemiluminescence detection system (Cell Signaling, MA, USA) on a LAS-3000 (Fuji, Japan).
34. Effects of the compounds on cell cycles of Ty-82 cell line were analyzed by using DNA-selective stain and NucleoCounter NC-250 system (Chemometec, Denmark). Briefly, cells were seeded at a density of 20,000 cells/well to the wells of 6 well plates and treated with compounds and incubated for 24 hrs. Subsequently, cells were resuspended in a lysis buffer containing nuclear stain dye DAPI and incubated for 5 min. Then the cells were further treated with stabilization buffer provided by the company and quantify DNA content of the cells allowing determination of cell cycle phases.
35. Full BROMOscan™ data of compound 13 is available in the supplementary material.

Supplementary Material

Compound 13 BROMOscan™ data and NMR spectra of selected compounds are attached in the supplementary material.